

Is the density of electron charge a statistical quantity?

Werner A. Hofer

Department of Physics, The University of Liverpool, Liverpool, L69 3BX, UK.

Abstract:

We show by a statistical analysis of high-resolution scanning tunneling microscopy (STM) experiments, that the interpretation of the density of electron charge as a statistical quantity leads to a contradiction with the energy conservation principle. Given the precision in these experiments we find that the electron energy has to be more than three orders of magnitude larger than the band energy of surface electrons. We are thus forced to conclude that the density of electron charge is a physically real, i.e. in principle precisely measurable quantity, as derived in a recent paper.

Keywords: electron charge, scanning tunneling microscope, quantum theory

In density functional theory (DFT) a many-electron system is comprehensively described by the density of electron charge (Hohenberg & Kohn 1964, Kohn & Sham 1965). However, the density itself, within the framework of second quantization, is thought to be a statistical quantity (Born 1926a, Born 1926b). In principle, this statement can be tested by a statistical analysis of high-resolution STM measurements including the uncertainty relations (Heisenberg 1927).

Today, STMs have reached a level of precision which is quite astonishing. While it was barely possible to resolve the positions of single atoms in early experiments (Binnig *et al.* 1982; Binnig & Rohrer 1987), it is now routine not only to resolve the atomic positions but also e.g. the standing wave pattern of surface state electrons (Heller *et al.* 1994) on metal surfaces, and even very subtle effects like inelastic excitations, Kondo resonances, or surface

charging (Gawronski *et al.* 2008, Neel *et al.* 2007, Harikumar *et al.* 2008). What the STM measures, in these experiments, is the current between a surface and a very sharp probe tip. The current itself is in most cases proportional to the density of electron charge at the surface (Hofer *et al.* 2003). From the viewpoint of a physicist of the golden age of quantum mechanics, say the time around 1925, this precision of measurements, where the vertical resolution of the best instruments is close to fifty times smaller (about 0.05 pm as Gawronski *et al.* showed 2010) than the Compton wavelength of an electron (or about 2.4 pm), must seem like magic. In Figure 1 we show a quantum corral of 51 silver atoms on an Ag(111) surface measured by Rieder *et al.* 2004. In some images the instrument was able to resolve not only the standing wave pattern of surface state electrons, but also the modulation due to the positions of single surface atoms. The measurement is quite spectacular, and it raises some very fundamental problems in quantum mechanics, which we shall explore in the following. It is irrelevant for this analysis, whether the remaining experimental imprecision is due to microscopic or macroscopic processes: it is the level of precision in these experiments itself, which is problematic.

It is difficult to define the *exact* uncertainty of momentum of a surface state electron in the experiments. From the energy resolution in today's best measurements of about 1 meV (Heinrich *et al.* 2004) one could infer an uncertainty of momentum $\Delta p = 1.52 \cdot 10^{-26}$ kgms⁻¹, and a local uncertainty $\Delta x = 3.1 \cdot 10^{-9}$ m, or 3.1 nm. However, to establish that the uncertainty relations fail in this context, it is only necessary to provide an upper limit of the energy and momentum uncertainty. Thus, for an electron at the Fermi level of a Ag(111) surface the maximum available energy is given by the energy difference between the bottom of the parabolic surface state band and the energy at the Fermi level. This energy is about 80 meV. This corresponds also to the thermal energy at ambient conditions. As the experiments are performed at cryogenic temperatures of 5K, the thermal energy is much lower than the band energy. Hence the maximum uncertainty in the energy of the electron is also about 80 meV. From this value it is possible, via the Heisenberg uncertainty relations $\Delta p \Delta x \geq \hbar/2$, to

derive the uncertainty of the x-position: $\Delta x = 3.48 \cdot 10^{-10}$ m or about 3.5 Å. This value is about three times larger than the Wigner-Seitz radius (1.06 Å), which describes the radius of a sphere with the typical electron density found in metals. The uncertainty Δx is also larger than the distance between two individual atoms on a silver surface, which is 2.9 Å. The unit cell, the Wigner Seitz cell, and the uncertainty are marked in Figure 1c.

Following the standard interpretation of quantum theory the electron is a point particle. Its appearance at a particular location is a statistical event governed by the Schrödinger equation and the probability density, which is equal to the square of the electron's wavefunction, or $\psi^* \psi$. The same statement is also correct for alternative interpretations of quantum mechanics, e.g. based either on the pilot-wave theory (de Broglie 1960, Bohm 1952a, Bohm 1952b), or a theory of the Dirac electron based on Zitterbewegung (Hestenes 2010). In this case the precision of an experiment will depend on the statistical variation of the electron's location and its convolution over time. This, however, will also influence the statistical variation of e.g. the apparent height. If the apparent height can be measured with the precision of less than 0.05pm, as found in experiments (Gawronski *et al.* 2010), then the statistical probability of an electron to be found at a particular location can only have a certain standard deviation. Given the local uncertainty derived from the uncertainty relations, and assuming that the standard deviation decreases with an increase of the number of measurements, this deviation can be linked to a minimum number of events within the measurement interval of an STM, which is in the range of milliseconds. The number of measurement points within the Wigner-Seitz cell is known, given the lateral resolution of and STM in the range of about 10pm. Consequently, we can determine the average number of times an electron must be detected at a measurement point in a certain interval. Given the size of the Wigner-Seitz cell, we can also calculate the average velocity of the electron between measurements, the quantum mechanical velocity of the electron under the given measurement conditions. If this velocity is substantially higher than allowed for by the electron's energy, or if the minimum standard deviation found in the experiments is substantially smaller than allowed for by the electron's energy, then one of the original assumptions going into the analysis of the process must be flawed. We show that this

is indeed the case.

In the following we start the discussion by analyzing events at one particular pixel of the grid on the surface and analyze events from the viewpoint of one electron only. Subsequently, we shall determine how the presence of many electrons at the surface could alter the initial findings.

The apparent height of a feature measured by STM is, for a metal surface, in the range of 10 to 200pm. For the sake of the argument, and to avoid being overly restrictive, we assume the vertical resolution to be 0.1pm, and the lateral resolution to be 20pm. In a Wigner-Seitz cell we then have about 88 individual pixels of STM measurements (see Figure 1d). If we assume that the feature height is 30pm, then the experimental precision is 0.3%. The apparent height at an individual pixel would be affected, however, if at a given moment during the measurement interval the electron were not found at the location of this pixel, but at a neighboring pixel. Thus we may say that the standard deviation of the location measurement is such that the required percentage of measurements must be at this particular location. For a variation of less than 0.3% three times the standard deviation of the measured results must thus still be smaller than half the distance between the pixels (see Figure 1d), or about 10pm. The standard deviation must thus be smaller than 3.3pm. Given that the uncertainty $\Delta x = 348$ pm, every single measurement event, at which the electron should be detected at the position of one pixel at $(x, y) = (0, 0)$, will lead to a statistically distributed measurement in the interval $-348 < x < +348$, and $-348 < y < 348$. We have simulated such a statistical distribution of events in Figure 2. It can be seen that the locations of the electron are indeed randomly distributed in the interval, as required by the uncertainty relations and quantum mechanics. We find a standard deviation of about 280pm for all sets of data. Increasing the number of measurements does not change the precision, since the precision is limited by the uncertainty relations themselves. The precision can only be increased by an increase of the electron's energy. Since σ is about one hundred times the required value, we may say that there is a clear contradiction between the observed precision of the experiments, and the

calculated uncertainty for the location of the electron. It is also clear that the underlying assumption, leading to this contradiction, is the statistical nature of the measurement, encoded in the uncertainty relations. This contradiction, moreover, is not the result of a small variation of the values obtained, but a variation of two orders of magnitude.

It is straightforward to calculate the energy necessary to obtain the precision found in the experiments. If σ has to be around 3pm, then the necessary uncertainty Δx will also be about 3pm. This means that the momentum uncertainty has to be around $1.76 \times 10^{-23} \text{kgms}^{-1}$, and the necessary energy will be more than 1000eV. For a measurement taken at cryogenic temperatures of 5K, as routinely performed today, the probability of such energy, derived from the Fermi-Dirac distribution, is essentially zero; the precision found in the experiments is thus impossible to explain within the framework of standard quantum theory.

The result would not change substantially if the precision in the experiments were somewhat lower. However, so far we have assumed that the uncertainty leads to a *loss* of electron detection at a particular point. It is, at least in principle, also possible, that uncertainty, via the influx of adjacent electrons at this particular point, may lead to a *gain* in electron detection. We may calculate this gain from the normal distribution for the distance from adjacent pixels and the ratio of the diameter of a pixel, or 20pm and the circumference of a circle at this distance, so that the normalized gain from a point at distance d will be (units in pm):

$$g(d) = \frac{20}{2\pi d} \frac{1}{\sqrt{2\pi\sigma^2}} e^{-\frac{d^2}{2\sigma^2}} \quad (1)$$

Summing up all contributions from pixels in a distance d of less than 280 pm, we obtain a value of 0.65. For a contrast of 100, corresponding to an apparent height difference of 200pm, which is easily obtained in an STM, the gain at a particular pixel should not be larger than 0.01. Comparing with the number obtained from a normal distribution, based on a standard deviation of 280pm and a pixel width of 20pm, or 0.65, we see that such a contrast cannot be obtained if the density of charge is assumed to be a statistical quantity complying with the uncertainty relations. Again, the value obtained from the statistical analysis differs

by about two orders of magnitude from the value inferred from the experiments. So that from both perspectives, the loss due to the appearance of the electron at adjacent pixels, and the gain due to the appearance of the electron statistically deviating from adjacent pixels, we arrive at the same conclusion: the precision and contrast of today's STM experiments is well beyond the requirements of the uncertainty principle. It is thus safe to conclude that the density of charge *cannot be* a statistical quantity.

To show in detail, how a statistical density of electron charge complying with the uncertainty relations would affect the image of a single adatom at the silver surface, we have simulated the image of an adatom at very low bias voltage (20mV), in constant height mode at a distance of 500pm above the centre of the adatom. Figure 3 shows two possible images: Figure 3a reflects a non-statistical measurement, where the measured current is exactly proportional to the calculated local density of states (LDOS), this image is very close to experimental results (see Fig. 1a, and the measurements by Lian *et al.* 2010). Figure 3b shows a hypothetical measurement, where the LDOS value at every single point is affected by the random distribution of the electrons present at a given point. In this image we have summed up all contributions from the normal distributions of adjacent measurement points, where the amplitude is equal to the exact density of states at a given point, and its contribution to adjacent points is calculated from a normal distribution with a standard deviation of 280pm. We have rescaled the ensuing LDOS values to the maximum value for the density. Figure 3c shows a simulated linescan across a single adatom. Here, the numerical difference is more than one order of magnitude. The simulation allows the conclusion that measurements of adatoms would not be able to show an apparent height difference of more than about 10pm. This is, again, a clear contradiction with experimental results, where the apparent heights are typically larger than 100pm.

These findings take us back about eighty years to the original development of modern physics. At this point, two different approaches to atomic physics were proposed: one, by Heisenberg, Born and Jordan, based on matrices and classical mechanics; the other, by de Broglie and Schrödinger, based on wave properties and an adaptation of classical

electrodynamics. The rift between these two approaches had repercussions in the development of physics for at least two generations. Today, both approaches are combined in our modern quantum theory. However, it was recently shown that a model of extended electrons, which is more in line with Schrödinger's than Heisenberg's concept, can remove some of the main obstacles to an understanding in atomic scale physics (Hofer 2011). The model is sketched in Figure 4. It has the following advantages: (i) The self-energy, which would be infinite for a point-like electron, is calculated to be typically 8.16eV; it can be accounted for by a simple density-dependent cohesive potential. (ii) The spin $\mathbf{S} = S \mathbf{e}_v$ of a free electron is a vector quantity directed either parallel or anti-parallel to the velocity vector \mathbf{v} , it changes in an external and time-dependent magnetic field \mathbf{B} according to a modified Landau-Lifshitz equation:

$$\frac{d\mathbf{S}}{dt} = \alpha \cdot \mathbf{S} \times \mathbf{B} + \beta \cdot \mathbf{S} \times \left(\mathbf{v} \times \frac{d\mathbf{B}}{dt} \right) \quad (2)$$

where α and β are constants. A statistical manifold of spin-up and spin-down electrons in a constrained trajectory of the electron as e.g. within the Coulomb field of a nucleus in this case yields exactly two results in a Stern-Gerlach type experiment. (iii) The electron density is a real physical quantity, it varies with time and space in the wave-propagation of the electron and it can be shown how it changes due to accelerations. (iv) The wavefunction is not strictly a physical property of electrons, since it combines density components and field components in one (a multivector) structure. Therefore effects like the notorious spreading of the wavepacket for free electrons are mere artifacts within this new model and without physical reality. (v) While in standard theory the stability of hydrogen is referred to the uncertainty principle (which prevents that the electron falls into the nucleus), in the model of extended electrons it is the requirement that the energy density within one electron has to be constant, which prevents this outcome. (vi) While there is a strict divide between atomic-scale physics and macro physics in the standard framework, due to the necessary integrations over infinite space if one is to calculate a measured value, this divide vanishes in the new framework: a consistent theoretical framework can thus be constructed from the nanometer to the meter scale.

In the present context, what the STM will measure, is the intrinsic density distribution of single surface electrons, which are spread-out into their lateral Wigner-Seitz cells. The measurements in this case can be arbitrarily precise: since the density is a physical, and not merely a statistical quantity, there is no limit to the precision in a measurement. Given the conceptual advantages of the model, and the fact that a statistical approach does violate the uncertainty principle, as shown, we think it is time to reconsider the famous Heisenberg-Schrödinger controversy.

In summary, we have shown that modern STM experiments violate the Heisenberg uncertainty relations by about two orders of magnitude. This indicates that the density of electron charge is not a statistical quantity, as currently believed.

Acknowledgments

Helpful discussions with Krisztian Palotas are gratefully acknowledged. The author thanks the Royal Society London for support.

References

Binnig, G., Rohrer, H., Gerber, Ch., & Weibel, E. 1982 Surface Studies by Scanning Tunneling Microscopy, *Phys. Rev. Lett.* **49**, 57 - 61.

Binnig, G., & Rohrer, H. 1987 Scanning tunneling microscopy—from birth to adolescence, *Rev. Mod. Phys.* **59**, 615 – 625.

Born, M. 1926 Zur Quantenmechanik der Stoßvorgänge, *Zeitschr. f. Phys.* **37**, 863-867.

Born , M. 1926 Quantenmechanik der Stoßvorgänge, *Zeitschr. f. Phys.* **38**, 803-827.

Bohm, David. 1952 A Suggested Interpretation of the Quantum Theory in Terms of "Hidden" Variables I, *Phys. Rev.* **85**, 166–179.

Bohm, David. 1952 A Suggested Interpretation of the Quantum Theory in Terms of "Hidden" Variables II, *Phys. Rev.* **85**, 180–193.

De Broglie, L. 1960 Non-linear Wave Mechanics: A Causal Interpretation. Elsevier, Amsterdam.

Gawronski, H., Mehlhorn, M. & Morgenstern, K. 2008 Imaging Phonon Excitation with Atomic Resolution, *Science* **319**, 930-933.

Harikumar, K. R., Lim, T. B., McNab, I. R., Polanyi, J. C., Zotti, L., Ayissi, S. & Hofer, W. A. 2008 Dipole-directed assembly of lines of 1,5-dichloropentane on silicon substrates by displacement of surface charge, *Nature Nanotechnology* **3**, 222-228.

Heinrich, A. J., Gupta, J. A., Lutz, C. P., Eigler, D. M. 2004 Single-Atom Spin-Flip Spectroscopy, *Science* **306**, 466-469.

Heisenberg, W. 1927 Über den anschaulichen Inhalt der quantentheoretischen Kinematik und Mechanik, *Zeitschr. f. Phys.* **43**, 172 - 198.

Heller, E. J., Crommie, M. F, Lutz, C. P. & Eigler, D. M. 1994 Scattering and adsorption of surface electron waves in quantum corrals, *Nature* **394**, 464 - 466.

Hestenes, David. 2010 Zitterbewegung in Quantum Mechanics, *Found. Phys.* **40**, 1-54.

Hofer, W. A., Foster, A. S. & Shluger, A. L. 2003 Theories of scanning probe microscopes at the atomic scale, *Rev. Mod. Phys.* **75**, 1287 – 1331.

Hofer, Werner A. 2011 Unconventional Approach to Orbital-Free Density Functional Theory Derived from a Model of Extended Electrons, *Found. Phys.* **41**, 754 - 791.

Hohenberg, P. & Kohn, W. 1964 Inhomogeneous electron gas, *Phys. Rev.* **136**, B864 - B871.

Kohn, W. & Sham, L. J. 1965 Self-Consistent Equations Including Exchange and Correlation Effects, *Phys. Rev.* **140**, A1133 - A1138.

Lian, J. C. *et al.* 2010 Mapping antibonding electron states of a Pb adatom on Pb(111), *Phys. Rev. B* **81**, 195411-15.

Neel, N., Kroger, J., Limot, L., Palotas, K., Hofer, W. A. & Berndt, R. 2007 Conductance and Kondo effect in a controlled single-atom contact, *Phys. Rev. Lett.* **98**, 016801-04.

Rieder, K.-H., Meyer, G., Wai Hla, S., Morescu, F., Braun, K. F. Morgenstern, K., Repp, J., Foelsch, S. & Bartels, L. 2004 The scanning tunneling microscope as an operative tool: doing physics and chemistry with single atoms and molecules, *Phil. Trans. R. Soc. Lond. A* **362**, 1207 - 1216.

Figure Legends

Figure 1 (online version in colour): Quantum corral and surface state electron on a Ag(111) surface. **a** The propagation of the surface state electrons leads to periodic variations of the density and the apparent height. **b** In high-precision measurements these variations are modulated by the electronic structure of surface atoms. **c** Small region of the central image blown up and annotated: the unit cell, the area of a single electron, and the local uncertainty are marked. **d** The Wigner-Seitz cell of a single electron contains at least 88 pixels of measurements, if the lateral resolution is assumed to be 20pm. From Rieder *et al.* 2004.

Figure 2 (online version in colour): Random distribution of the location of a point-like electron on the surface. **a** 100 events, **b** 1000 events, **c** 10000 events. The standard deviation σ of the radius for each of the distributions is about 280 pm (random distribution taken from random.org).

Figure 3: Simulated constant height contour of silver adatom. **a** Simulation based on the exact values of the local density of electron charge. The contour is similar to the experimental results shown in Fig. 1 and to measurements and simulations of a Pb adatom presented in Ref. 18. **b** Simulation based on a convolution of probabilities for a standard deviation of 280pm. **c** Linescan across the adatom for both simulations. The exact values of the density yield an apparent height which is more than one order of magnitude higher than the apparent height in the simulation based on quantum statistics.

Figure 4 (online version in colour): Model of extended electrons. **a** The electron is an extended structure with a diameter of about 0.2 nm; the density of charge ρ and the spin density S are oscillating functions, their wavelength complies with the de Broglie relations. **b** In a constrained trajectory magnetic fields will lead to a rotation of the spin density vector:

the induced spin density is either parallel or antiparallel to the applied magnetic field.

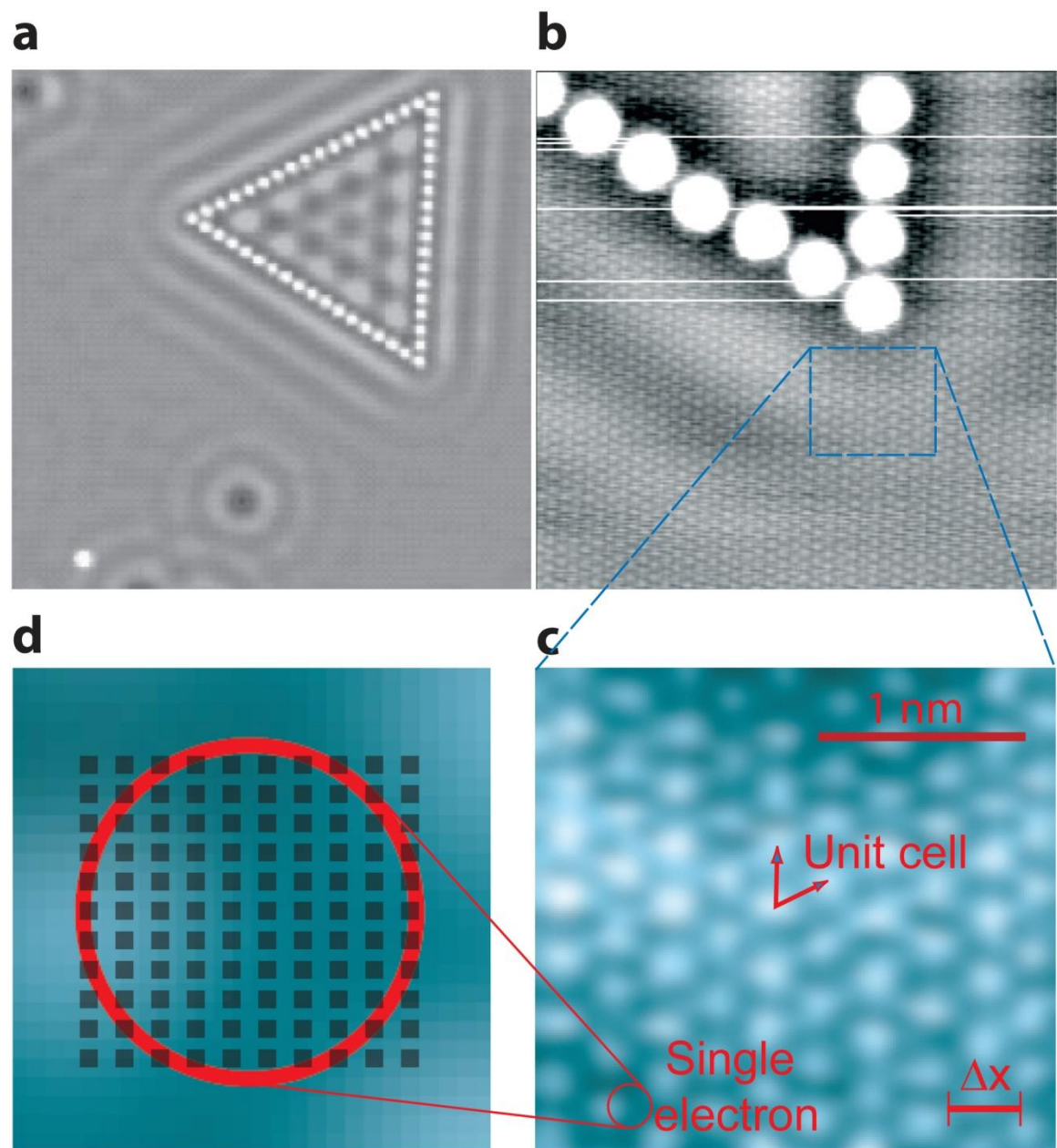


Figure 1

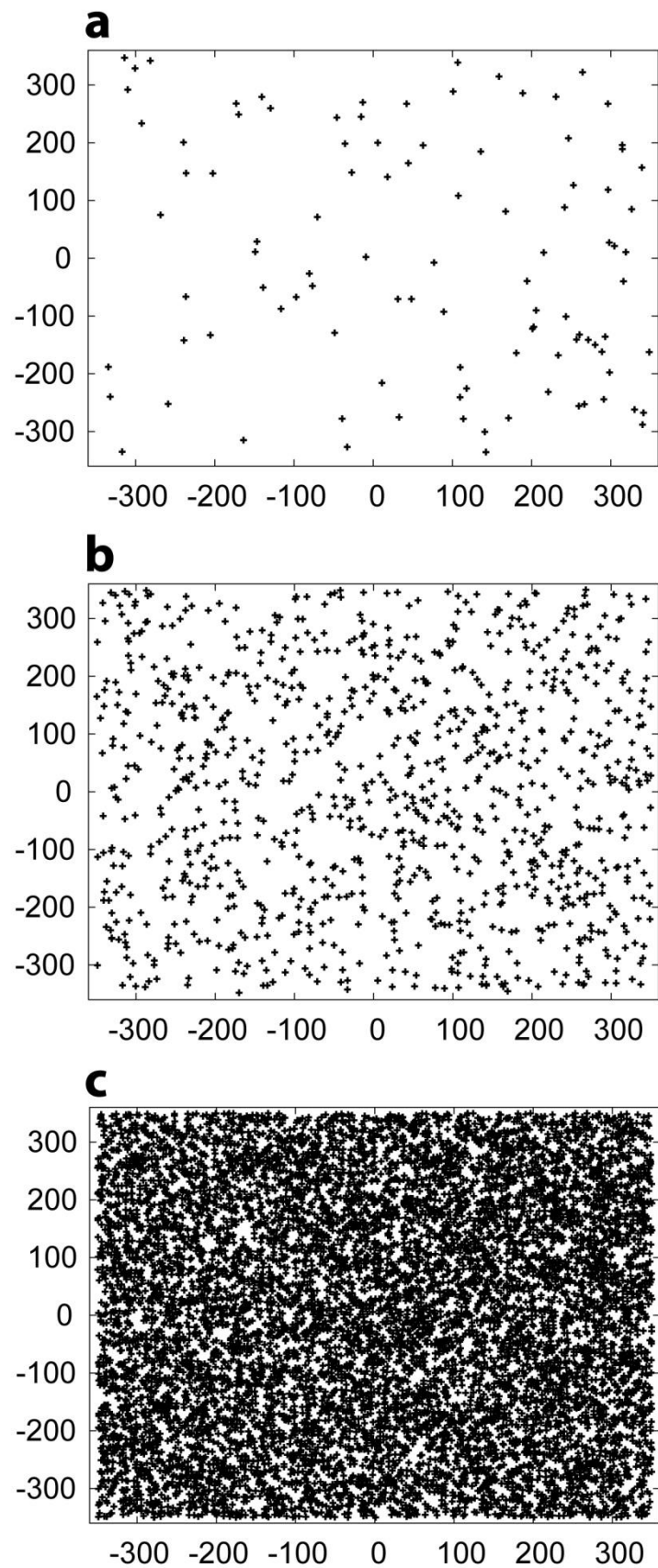


Figure 2

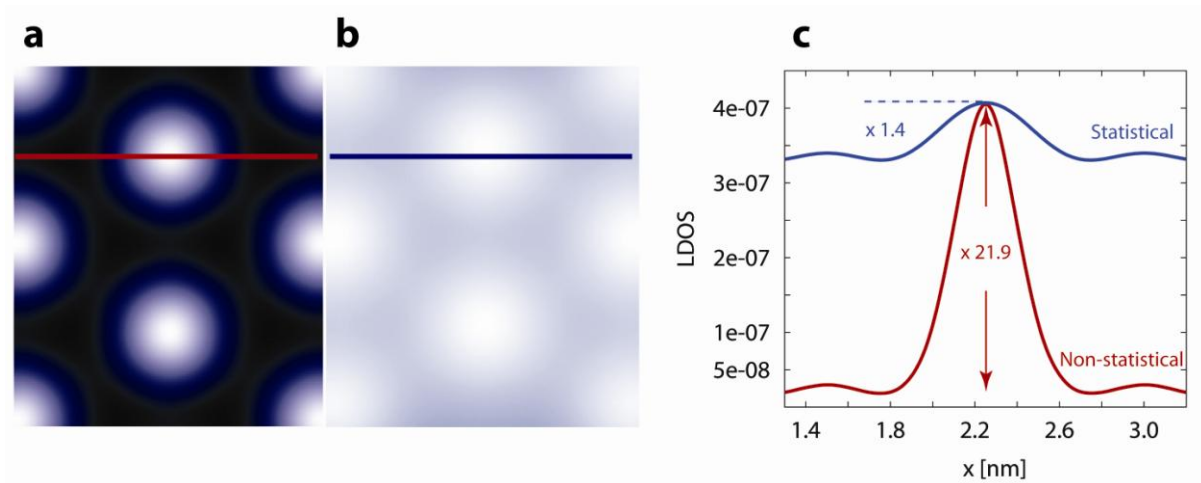


Figure 3

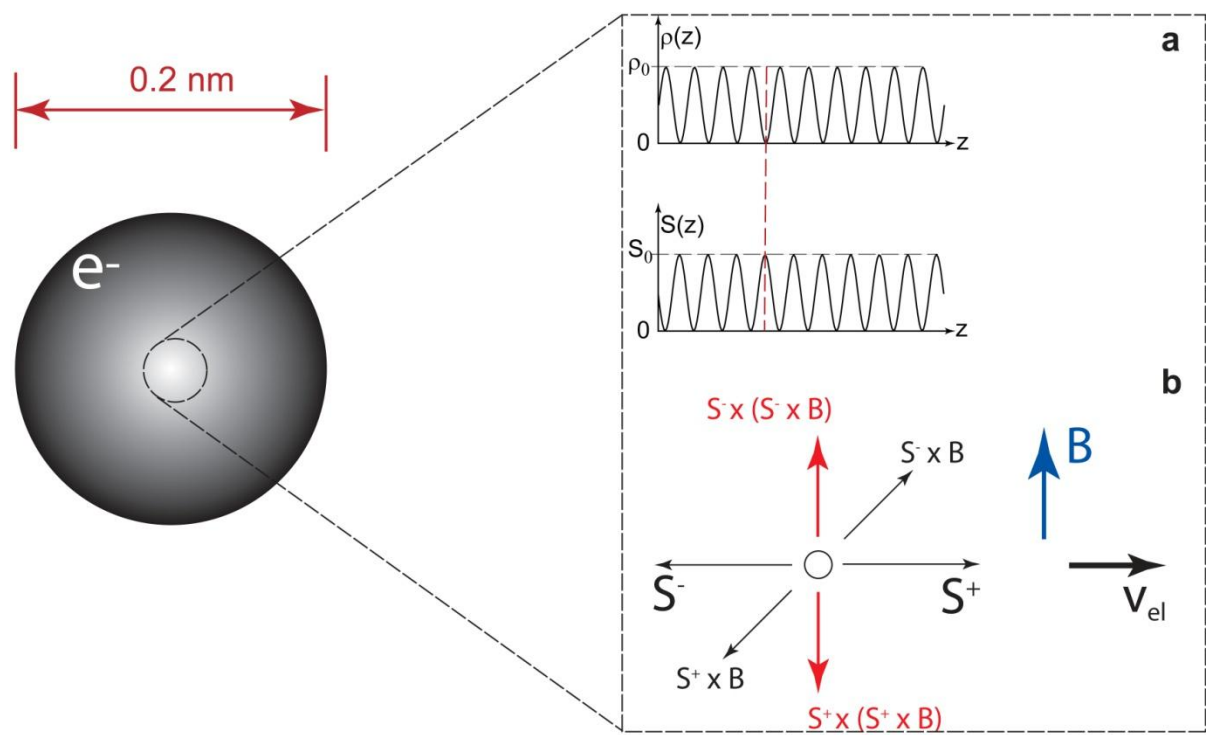


Figure 4